Fundamental and Overtone Vibrational Spectra of Gas-Phase Pyruvic Acid†

Kathryn L. Plath,‡,§ Kaito Takahashi,‡ Rex T. Skodje,*,‡ and Veronica Vaida*,‡,§

Department of Chemistry and Biochemistry, and CIRES, University of Colorado, Campus Box 215, Boulder, Colorado 80309

Received: December 4, 2008; Revised Manuscript Received: January 19, 2009

Pyruvic acid ($CH_3COCOOH$) is an important keto acid present in the atmosphere. In this study, the vibrational spectroscopy of gas-phase pyruvic acid has been investigated with special emphasis on the overtone transitions of the OH-stretch, with $\Delta v_{OH} = 2, 4, 5$. Assignments were made to fundamental and combination bands in the mid-IR. The two lowest energy rotational conformers of pyruvic acid are clearly observed in the spectrum. The lowest energy conformer possesses an intramolecular hydrogen bond, while the next lowest rotational conformer does not. This difference is clearly seen in the spectra of the OH vibrational overtone transitions, and it is reflected in the anharmonicities of the OH-stretching modes for each conformer. The spectra of the OH-stretching vibration for both conformers were investigated to establish the effect of the hydrogen bond on frequency, intensity, and line width.

I. Introduction

It is well-known that infrared (IR) absorption spectroscopy can provide a wealth of information about the potential energy surface and the molecular structure of gas-phase species. Combining experimental observations with theoretical calculations, one can elucidate the structure, bond strengths, and frequencies of the absorbing molecule and also probe the mode−mode coupling that causes intramolecular energy transfer.

Pyruvic acid (PA), $CH_3COCOOH$, is an α-dicarbonyl that possesses conformers, which differ by the degree of intramolecular hydrogen bonding and can be effectively studied using absorption spectroscopy. PA is a prototype for atmospheric α-dicarbonyls and thus has been the subject of a considerable amount of research. Nevertheless, there is still insufficient quantitative information on its spectroscopic and chemical properties.[1] The fundamental transitions, in the range of 1000−5000 cm^{-1}, have been measured in the gas-phase and in a low temperature matrix.[2−4] Schellenberger et al.[3] performed the initial gas-phase work on the IR spectrum of PA. Hollenstein et al.[2] later reported the frequencies in gas-phase and in an argon matrix and performed the normal-mode analysis. We note the electronic spectroscopy of PA has also been investigated, including the $\pi^* \leftarrow$ n transition in the near-UV.[1,5] The UV cross sections and *J*-values of PA were reported; the results show that absorption spectrum peaks at approximately 355 nm and is negligible by 400 nm.[1]

The geometries of the PA conformers have been inferred from measurements of the microwave spectrum.[6,7] Reva et al.[4] investigated the spectroscopic features of the rotational conformers of PA in the IR, which have also been studied theoretically.[4,8−13] The two lowest energy conformers of PA are separated by 2.08 kcal/mol, while the other conformers lie much higher in energy.[4,6,7,12] As shown in Figure 1, the second lowest conformer has the acidic hydrogen rotated away from the ketonic oxygen, while the most stable conformer forms an intramolecular hydrogen bond between the acidic hydrogen and the α-carbonyl. The lowest energy conformer is labeled as the trans−cis (Tc) conformer, and the higher energy conformer is the trans−trans (Tt). The Tt conformer is close enough in energy to the most stable Tc conformer that significant thermal population is possible at ambient temperatures. Both conformers are observed in this study, allowing an investigation of the effect of hydrogen bonding on the OH vibrational spectrum.

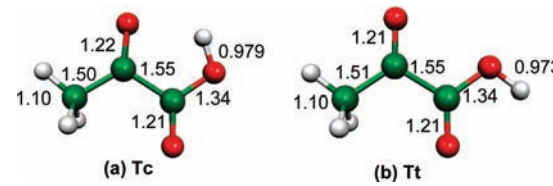

Figure 1. Schematic diagram of (a) Tc and (b) Tt conformers of pyruvic acid. The optimized bond lengths in angstroms are listed along the bonds, with only one value listed for the three CH bonds.

Intra- and intermolecular hydrogen bonds[14−16] can form in carboxylic acids, generally with bond strengths between 5 and 10 kcal/mol. Intramolecular hydrogen bonds form in some difunctionalized compounds, such as PA, and significantly alter the potential energy curve of the OH-stretching vibrational mode. Glycolic acid, diols, catechol, malonic acid, and many others are also known to form an intramolecular hydrogen bond.[17−23] The intramolecular hydrogen bond has a strong effect on the frequency and intensity of the OH vibrational stretching transition by altering the OH bond length and strength.[19,24] Hydrogen bonded interactions and their effects on vibrational spectroscopy have been explored extensively, in particular their consequences in biological systems.[25−28] The effects of the intramolecular hydrogen bond of PA on the potential energy surface are addressed in this study by way of vibrational spectroscopy.

The OH-stretching vibrational mode is high in frequency (∼3500 cm^{-1}) and has a large anharmonicity. This large anharmonicity accounts for the relatively large intensity of its overtone transitions. The high frequency of the OH-stretching mode and relatively large overtone intensities allow excitation

† Part of the "Robert Benny Gerber Festschrift".

* To whom correspondence should be addressed. (R.T.S.) Telephone: (303) 492-8194. Fax: (303) 492-5894. E-mail: Rex.Skodje@colorado.edu. (V.V.) Telephone: (303) 492-1422. Fax: (303) 492-5894. E-mail:Vaida@colorado.edu.

‡ Department of Chemistry and Biochemistry.

§ CIRES.

10.1021/jp810687t CCC: $40.75
Published on Web 03/04/2009

to chemically relevant energies. Overtone spectroscopy accesses the higher energy region of the potential energy surface to reveal the deviations from a harmonic potential. Because the overtones are particularly sensitive to bond changes, overtone spectroscopy is an excellent method to extract information on the molecular properties in the anharmonic part of the ground electronic state potential energy surface.[29−33]

In this work, we sought to gain insight into the potential energy surface of the two conformers of PA through the absorption spectrum. Subtle changes in the frequency of the carbonyl stretching modes and OH-stretching modes reflect structural differences as well as changes in the potential energy surfaces. The overtones of the OH-stretching modes are ideal transitions to highlight variances in the bond properties of multiple conformers of PA. Additionally, the occurrence of combination bands illustrates the energy transfer possible between the vibrational modes. The vibrational spectrum of PA is used to understand the effect of the intramolecular hydrogen bond on vibrational transitions at chemically relevant energies. Excitation of molecules, such as PA, has been shown to lead to photochemical reactions on the molecule's ground electronic state. The reaction barrier for decarboxylation of a keto acid or dicarboxylic acid has been calculated between 25 and 50 kcal/mol;[21,34−36] the calculated reaction barrier of pyruvic acid is 38 kcal/mol.[8,9,36] The OH-stretch can reach this barrier with at least four quanta.[17−20,37−77] For the reaction to occur, the energy must transfer from the localized OH-stretching mode to the reaction coordinate. Light excitation of OH vibrational overtone transitions of PA has been shown to undergo very fast reaction initiated by hydrogen atom chattering.[36,78]

Determing the spectroscopic properties of PA and other similar organic acids is essential to understanding the role of these compounds in the atmosphere. PA has been found, both in the gas-phase and on aerosols, in several different environments.[79−88] It is emitted directly into the atmosphere and is considered an oxidation product of isoprene. While the mechanism is unclear, the main removal pathway from the troposphere is through ultraviolet photolysis. The reaction with OH radical is a minor atmospheric pathway.[1,5,10,12,88−95] As previously discussed by Takahashi et al.,[36] the overtone-induced reaction of PA is possible in the troposphere.[14,18,21,96−105]

II. Experimental Section

Using Fourier transform infrared (FTIR) spectroscopy and cavity ring-down (CRD) spectroscopy, we measured the absorption spectrum of PA from 1000 to 16 400 cm^{-1}. FTIR allowed for easy measurement of the lower energy transitions because of its large frequency range and ability to acquire excellent relative intensities. However, it does not have the sensitivity to observe the low intensity overtone transitions. On the other hand, CRD is able to observe the third and fourth overtones of the OH-stretching mode due to its much longer effective path length compared to traditional absorption spectroscopies such as FTIR. The two techniques complement each other well to give a full representation of vibrational transitions PA.

Fourier Transform Infrared Spectra. The mid- and near-infrared absorption spectrum of PA was measured between 1000 and 11 000 cm^{-1} using FTIR at 355 K. The Bruker IFS 66v/s instrument and sample chamber have been described previously.[16,69] The mid-IR spectra were taken using two setups: a flow cell and a static cell. While the flow cell allowed for a higher number density and accurate relative intensities, it is only in the static cell that absolute cross sections can be obtained. The flow cell has a path length of 75 cm. N_2 gas was bubbled through a liquid reservoir of PA to force the sample through the cell. The cell was wrapped in heating tape for temperature control. The 20.6 cm static cell was used at ambient temperature and pressure with a connected sample reservoir; the vapor pressure was allowed to equilibrate throughout the cell. The near-IR spectrum, from 6000 to 11 000 cm^{-1}, was measured only in the flow cell setup. Spectra in the flow cell were recorded at 1 cm^{-1} resolution, and the static cell spectra at 4 cm^{-1} resolution. The FTIR technique allows for the simultaneous measurement of all wavelengths of light, producing accurate relative intensities of the various peaks in the fundamental vibrational range as well as the first overtone of the OH-stretching mode.[106,107]

Cavity Ring-Down Spectra. The spectra collected between 12 500 and 16 400 cm^{-1} used pulsed CRD. CRD increases the interaction time of the light pulse and the sample,[48,108,109] since the effective path length is 30−50 km. While the increase in sensitivity is necessary to measure the third and higher overtones, the instrument is limited to wavelengths between 600 and 800 nm. The CRD setup has been described in detail previously.[18,48,60,70] The 97 cm glass cell with Teflon fittings was wrapped in heating tape to elevate the temperature inside the cell, as previously described.[60] All of the mirrors used in the CRD experiments were from Los Gatos Research Inc. and had a 1 m radius of curvature (all with peak mirror reflectivity, R, of >99.997%). The spectra in the range 12 500−14 000 cm^{-1}, corresponding to $\Delta v_{OH} = 4$, used mirrors that were centered at 13 160 cm^{-1}. These mirrors achieved a maximum time constant of ∼160 μs corresponding to an effective path length of ∼40 km at the experimental conditions. The $\Delta v_{OH} = 5$ spectra were not recorded at 300 K because the low number density at those temperatures combined with the lower cross section did not create a large enough signal; however, the transition was recorded at 333 and 355 K. Two sets of mirrors were necessary to observe the range between 14 700 and 16 700 cm^{-1}, needed for the $\Delta v_{OH} = 5$ transition of the OH-stretch. The 14 700−15 900 cm^{-1} spectra were acquired using mirrors centered at 15 150 cm^{-1}. This setup created a maximum time constant of ∼170 μs. Between 16 000 and 16 700 cm^{-1}, the spectra were collected using a third set of mirrors, centered at 16 400 cm^{-1} with a peak time constant of ∼100 μs.

Sample Preparation. Fluka supplied the PA sample (purity ≥ 98.0%). Prior to each use, the sample was dried overnight using molecular sieves to remove excess water. The vapor pressure of PA showed great discrepancy in the literature. It should be noted that the values reported by Stull are roughly 1 order of magnitude lower than the values presented by Macdonald et al. within our temperature region.[110,111] To resolve this discrepancy, we measured the vapor pressure at 300 K; our measurement used a low pressure volume of ∼50 millitorr, and we recorded the pressure created by a reservoir of liquid PA as 1.6 ± 0.2 torr. This value was in agreement with that of Stull[111] and was used for our integrated cross section determination. The number density of each conformer was obtained by multiplying the respective Boltzmann population ratio to the total number density of PA. The uncertainty in the cross section is based on the error in the intensity, which is approximately ±0.13, the temperature ($\Delta T = \pm 1$ K), and the vapor pressure (±0.2 torr).

III. Theory and Calculations

The structures of the two most stable conformers of PA were calculated by the hybrid density functional theory method using the B3LYP[112,113] functional with the 6-31+G(d,p) basis set,[114−118] and also by MP2[119] with aug-cc-pVTZ[120−122] employing the

TABLE 1: Transition Frequencies and Line Widths in the Mid-IR Vapor-Phase Spectrum of Pyruvic Acid[a]

mode	mode description	exptl frequency (cm^{-1})	lit. frequency[2] (cm^{-1})	calcd frequency[4] (cm^{-1})	calcd intensity[4] (cm/molecule)	fwhm (cm^{-1})
υ_{24}	C−C torsion		90	94	1.16×10^{-18}	
υ_{23}	CH_3 torsion		134	135	1.66×10^{-20}	
υ_{16}	CCC bend			246	4.03×10^{-18}	
υ_{15}	CCO bend			384	1.56×10^{-18}	
υ_{22}	C═O ketone rock		392	386	2.61×10^{-18}	
υ_{14}	C═O acid bend			521	4.98×10^{-19}	
υ_{13}	C-O ketone bend		604	596	2.72×10^{-18}	
υ_{21}	OH torsion		668	686	1.09×10^{-17}	
υ_{20}	C−C symmetric stretch			730	4.48×10^{-18}	
υ_{12}	C═O acid rock		761	762	1.99×10^{-18}	
υ_{11}	CH_3 rock (A′)		970	969	2.29×10^{-18}	
υ_{19}	CH_3 rock (A″)	1030	1021	1015	1.66×10^{-19}	46
υ_{10}	C−O stretch	1133	1134	1139	9.20×10^{-18}	30
$\upsilon_9 (+ 2\upsilon_{13})$	COH bend	1211	1218	1245	1.74×10^{-17}	34
υ_8	CH_3 symmetric bend	1360	1360	1357	3.68×10^{-17}	30
υ_7	C−C asymmetric stretch	1391	1390	1397	1.54×10^{-17}	35
υ_6	CH_3 asymmetric bend (A′)	1424	1422	1439	1.69×10^{-18}	37
υ_{18}	CH_3 asymmetric bend (A″)			1431	1.94×10^{-18}	
υ_5	C═O ketone stretch	1737	1733	1715	1.08×10^{-17}	36
υ_4	C═O acid stretch	1804	1805	1791	3.21×10^{-17}	29
υ_3	CH_3 symmetric stretch	2941	2932	2955	6.64×10^{-20}	42
υ_2	CH_3 asymmetric stretch (A′)	3025	3027	3085	6.31×10^{-19}	29
υ_{17}	CH_3 stretch (A″)			3037	6.64×10^{-20}	
υ_1 (Tc)	O−H stretch	3463	3463	3467	1.96×10^{-17}	36
υ_1 (Tt)	O−H stretch	3579		3582	1.49×10^{-17}	68

[a] The experimental frequencies have an error of ± 4 cm^{-1}. The literature frequencies in the vapor phase are as reported by Hollenstein et al.[2] The calculated frequencies and intensities are from the results of Reva et al.[4]

Gaussian 03 program.[116] The optimized bond lengths from the MP2 method are given in Figure 1. It can be seen that the hydrogen bonding in the stable Tc conformer causes an elongation of the OH bond compared to the Tt conformer. The calculated frequencies and integrated cross sections are in agreement with the previous theoretical values reported by Reva et al.,[4] giving us confidence in these calculation methods.

For the theoretical calculation of the peak position and integrated cross section of the OH-stretching vibrational mode, we first used a one-dimensional local mode model[24,29,30,32,123−127] employing the potential energy curve and dipole moment function obtained at the B3LYP level. The accuracy of the B3LYP method was confirmed by performing the one-dimensional calculations using a potential energy curve calculated by CCSD(T)[128,129]/6-311++G(3df,3pd)[114−118] along with a dipole moment function produced by CCSD[128]/6-311++G-(3df,3pd)[114−118] with the MOLPRO[130] program. The dipole moments for the CCSD calculations were performed without orbital relaxation. In the calculations using the coupled cluster method, we used the equilibrium geometry calculated by the MP2 method described above.

Initial calculations based on the one-dimensional OH-stretching local mode model[29,30,32,123] revealed the need for the inclusion of coupling to other normal modes in order to accurately reproduce the experimental spectra of higher overtones. We therefore performed a three-dimensional vibrational calculation including two in plane frame bending modes with fundamental frequencies of 251 and 390 cm^{-1} for the Tc conformer, and 248 and 388 cm^{-1} for the Tt conformer (modes υ_{15} and υ_{16} in Table 1).[36] The three-dimensional vibrational model, which explicitly included the potential coupling, was solved using the variational method with harmonic oscillator basis functions. The basis set consisted of 20 functions for the OH-stretching mode and 15 functions each for the two frame bending normal modes. The potential energy and dipole moment matrix elements were obtained from Gauss−Hermite integration with 40 points for the OH-stretching mode and 30 points each for the two frame bending modes. Using the B3LYP method, we calculated the potential energy and the dipole moments for the 36 000 grid points of (R_{OH},Q_{15},Q_{16}) while keeping the remaining normal modes fixed at their respective equilibrium values.

For the calculation of the homogeneous width of the spectra, we used a direct "on-the-fly" dynamics calculation employing our previously reported method using the B3LYP method.[105] From the exponential decay time of the classical analog of the autocorrelation function, we obtained the full width at half-maximum (fwhm) through the uncertainty principle. The inhomogenous width from the rotational envelope was estimated to be 35 cm^{-1}, and the sum of the homogeneous and inhomogenous widths was used to simulate the spectra by a Lorentzian line shape function. Using the Boltzmann populations of the two conformers along with the results for the peak positions, integrated cross sections, and full width at half-maximum for each conformer, we simulated the OH-stretching transitions in the spectra for $\Delta\upsilon_{OH} = 1, 2, 4$. Further details on the theoretical calculation methods are reported in Takahashi et al.[36]

IV. Results and Discussion

This work re-examines the previously published fundamental vibrational spectrum of PA[2−4] and extends the spectroscopic study up to 16 ,400 cm^{-1} with a focus on the combination bands and OH vibrational stretching overtones. PA has 24 normal modes, all of which are IR active and have been seen in the low temperature matrix;[4] however, only 20 of the modes have been identified in the gas phase.[2] We clearly observe 11 of the fundamental modes in the region from 1000 to 16 400 cm^{-1}. The mid-IR spectrum, obtained by FTIR, can be seen in Figure 2. Table 1 compares the previously reported experimental and theoretical values of the fundamental vibrational transitions with the present experimentally recorded data. Additionally, we

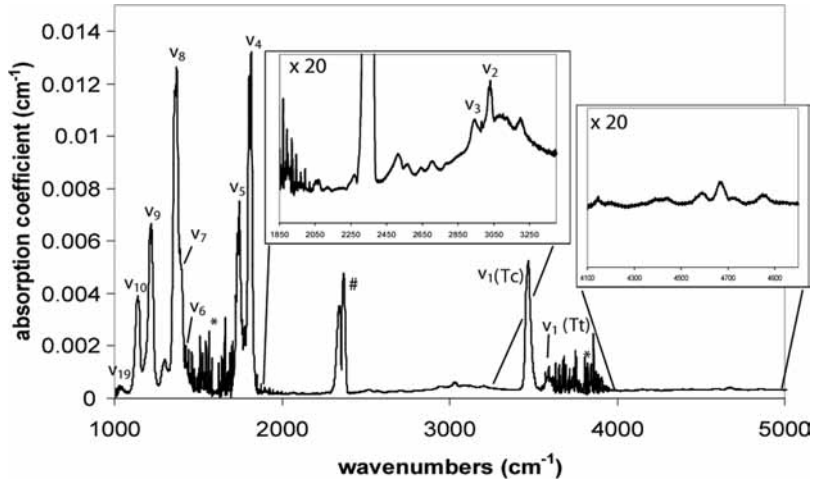

Figure 2. Observed vapor-phase FTIR spectra of pyruvic acid between 1000 and 5000 cm^{-1}. The fundamental transitions are labeled by the mode numbers. Some of the combination bands are magnified in the insets. (*) indicates water vapor impurity, and (#) is CO_2 impurity. The spectrum was recorded at 355 K.

TABLE 2: Assignments for Observed Combination Bands: Frequencies and Line Widths

mode	exptl frequency (cm^{-1})	fwhm (cm^{-1})
$\upsilon_{10} + \upsilon_{24}$	1224	
$\upsilon_9 + \upsilon_{24}$	1296	35
$\upsilon_4 + \upsilon_{24}$	1891	52
$\upsilon_8 + \upsilon_{13}$	1966	54
$\upsilon_4 + \upsilon_{16}$	2062	37
$\upsilon_8 + \upsilon_{12}$	2119	38
$\upsilon_9 + \upsilon_{11}$	2178	65
$\upsilon_5 + \upsilon_{14}$ or $2\upsilon_{10}$	2268	29
$\upsilon_4 + \upsilon_{20}$	2515	48
$\upsilon_8 + \upsilon_9$	2565	31
$\upsilon_9 + \upsilon_6$	2642	25
$\upsilon_5 + \upsilon_{11}$	2704	37
$\upsilon_4 + \upsilon_7$	3199	28
$\upsilon_3 + \upsilon_9$	4145	28
$\upsilon_1 + \upsilon_{20}$	4200	79
$\upsilon_1 + \upsilon_{11}$	4418	90
$\upsilon_1 + \upsilon_{10}$	4589	49
$\upsilon_1 + \upsilon_9$	4668	40
$\upsilon_3 + \upsilon_4$	4729	60
$\upsilon_1 + \upsilon_7$	4851	40

tentatively assign the combination bands in the range of 1000−8000 cm^{-1}. The data for these transitions are summarized in Tables 1 and 2. To the best of our knowledge, the cross sections and line widths of the fundamental vibrational transitions that we report have not been measured previously. Many of the transitions are not completely resolved from one another, making it impossible to directly measure accurate intensities. In an attempt to quantify these overlapping transitions, we used a superposition of Gaussian line shapes to fit these portions of the spectrum and obtain positions, integrated intensities, and fwhm values of the individual peaks. The majority of the bands are within a factor of 2, in agreement between the theory and experimental values. Figure 3 represents a comparison between our theoretical results and experimental findings of the OH-stretching transitions; the data for the OH-stretches is compiled in Table 3.

Identification of Conformers. At the experimental temperatures (300 and 355 K), both the Tt and Tc conformers (shown in Figure 1) are sufficiently populated to be observable in the fundamental and the overtone spectra. As seen in Figures 2 and 3, the OH-stretch fundamental and overtone transitions give rise to closely spaced doublets. Consistent with its lower thermal population, the high energy Tt-peak is smaller than the low energy Tc-peak. The intramolecular hydrogen bonding present in the lowest energy conformer (Tc) should "soften" the vibrational potential along the OH-stretch, thus lowering its frequency compared to the Tt conformer. Indeed, the fundamental frequency of the OH-stretch is observed to be about 120 cm^{-1} lower for the Tc conformer and is a clear fingerprint of the hydrogen bonding.[31] The potential energy curve of a hydrogen bonded OH-stretching mode deviates strongly from a free OH vibrational stretch. Thus, in addition to the frequency shift at the bottom of the potential well, there will also be large deviations of the potential curve from the Morse-like curve of the free OH as the H-atoms become closer to the ketonic oxygen atom. Thus, for the overtones of the OH-stretch, the difference in anharmonicity between the two conformers becomes more apparent and the transitions spread further apart in energy.[131] To a lesser extent, the C═O stretching modes can also reveal the structural differences between the two conformers due to the hydrogen bond. Studying the combination bands can also yield information regarding the potential energy surface of the excited O−H stretching states.

The distinction between the Tc and Tt conformers was also analyzed theoretically. The peak positions and intensities obtained for the one-dimensional vibrational calculation with the B3LYP methods are shown in Table 4, while those of CCSD(T) are given in Table 5. In Table 6, the three-dimensional results for the pure OH-stretching mode excitations, ($\Delta\upsilon_{OH}$, $\Delta\upsilon_{15}$, $\Delta\upsilon_{16}$) = ($\Delta\upsilon_{OH}$,0,0), and the pertinent combination bands, ($\Delta\upsilon_{OH}$,1,0) and ($\Delta\upsilon_{OH}$,0,1), are shown. The simulated spectra are shown in Figure 2 along with the experimental results. Comparing the results for the two levels of quantum chemistry presented in Tables 4 and 5, we find the peak positions obtained with B3LYP are lower than the more accurate CCSD(T) results by 40−200 cm^{-1}. On the other hand, the splitting between the Tc and Tt conformers was found to be remarkably similar between the two methods. In the intensity results, both quantum chemistry methods agree for the fundamental transition, while the overtones are overestimated by a factor of 2 in the B3LYP method. However, as shown in the sixth column of Tables 4 and 5, the ratio between the OH-stretching transitions of the Tc and Tt conformers is clearly reproduced, giving us confidence in using the B3LYP method to give the relative intensity of the two conformers in the three-dimensional model. Note that the sum of the absorption cross sections of the pure and two

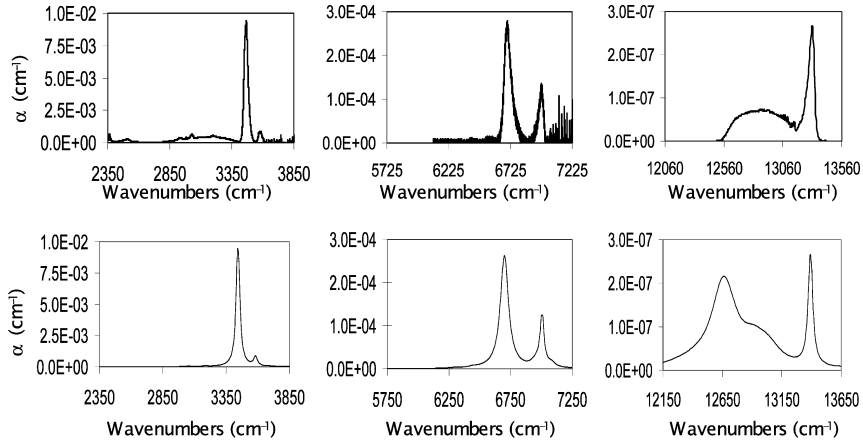

Figure 3. Spectrum of OH-stretch transitions. The top panels depict the experimental result for the fundamental transition, the first overtone, and the third overtone. Both conformers are observed in each panel. The bottom panels are the theoretical results for the corresponding transitions. The results are reported in terms of absorption coefficient, α (cm^{-1}), the product of the number density, and the absorption cross section. These spectra were recorded at 355 K.

TABLE 3: Observed Frequencies and Widths with the Theoretical Results of the O−H Stretching Transitions $0 \rightarrow v^a$

		Tc conformer				Tt conformer			
v	T (K)	exptl frequency (cm^{-1})	calcd frequency (cm^{-1})	exptl fwhm (cm^{-1})	calcd fwhm (cm^{-1})	exptl frequency (cm^{-1})	calcd frequency (cm^{-1})	exptl fwhm (cm^{-1})	calcd fwhm (cm^{-1})
1	358	3467	3445	37	35	3579	3583	64	35
2	358	6696	6702	69	79	6975	7007	71	38
4	355	12 920	12 663	414	247	13 311	13 394	56	46
5	355		15 401		366	16 237	16 375	78	58

[a] The theoretical frequencies were obtained using the 3D model of vibrational dynamics. The theoretical widths were obtained from dynamical simulation (ref 36).

TABLE 4: Peak Positions and Integrated Cross Sections Calculated by the 1D Local Mode Model (B3LYP/ 6-31+G(d,p)

v_{OH}	frequency (cm^{-1})	int cross section (cm/molecule)	frequency (cm^{-1})	int cross section (cm/molecule)	Tc/Tt int abs
1	3457	1.90×10^{-17}	3585	1.13×10^{-17}	169%
2	6739	5.74×10^{-19}	7011	8.94×10^{-19}	64%
3	9849	4.03×10^{-20}	10 282	5.16×10^{-20}	78%
4	12 794	3.64×10^{-21}	13 402	4.34×10^{-21}	84%
5	15 577	4.59×10^{-22}	16 374	5.00×10^{-22}	92%

TABLE 5: Peak Positions and Absorption Intensities Calculated by the 1D Local Mode Model (CCSD(T)/ 6-311++G(3df,3pd) Potential Energy Curve and CCSD/ 6-311++G(3df,3pd) Dipole Moment Functions)

v_{OH}	frequency (cm^{-1})	int cross section (cm/molecule)	frequency (cm^{-1})	int cross section (cm/molecule)	Tc/Tt int abs
1	3502	1.90×10^{-17}	3626	1.06×10^{-17}	179%
2	6824	3.49×10^{-19}	7087	5.49×10^{-19}	64%
3	9973	2.14×10^{-20}	10 389	2.49×10^{-20}	86%
4	12 953	2.07×10^{-21}	13 536	1.98×10^{-21}	105%
5	15 770	3.03×10^{-22}	16 530	2.57×10^{-22}	118%

combination transitions at each Δv_{OH} in the three-dimensional calculation is nearly equal to the one-dimensional results for the overtone transitions, consistent with the usual idea of intensity sharing.

Fundamental Carbonyl Stretching Transitions. Pyruvic acid contains two carbonyl functional groups, which have distinct C═O stretching vibrational frequencies. The ketonic carbonyl (v_5) is found to have a lower frequency centered at 1737 cm^{-1}, which agrees well with theory[4] and previous observation.[2,3] This mode appears as a doublet and can be seen in Figure 2, unobscured by a slight gas-phase water impurity on the lower energy side of the transition. The ketonic carbonyl stretch has an integrated cross section of $1.0 \pm 0.1 \times 10^{-17}$ cm/molecule, which reflects its large intensity in the spectrum.

The higher energy carbonyl stretch is that of the acid group (v_4) with a frequency centered at 1804 cm^{-1}. Previous work assigned this fundamental to the second overtone of the ketonic carbonyl bend (v_{13}) in resonance with the combination band $v_9 + v_{13}$.[2] This carbonyl stretch also appears with a doublet structure that Hollenstein et al. assigned as the P and R branches of rotation.[2] The acidic carbonyl stretch is the most intense feature in the spectrum and has an integrated cross section of $1.6 \pm 0.2 \times 10^{-17}$ cm/molecule. The large intensity of the transitions and strength of the C═O bond make the hydrogen bond effects more difficult to observe or quantify.

The ketonic C═O stretch does show a marked perturbation between the two conformers due to its involvement in the Tc conformer's hydrogen bond. The work of Eliason et al. reports that, for general carboxylic acid dimers, the C═O stretching mode is red-shifted by hydrogen bonding compared to the free C═O stretch.[16] This red-shift of the C═O stretching mode frequency for long chain organic acids was found to be approximately 70 cm^{-1}. In PA, the effect on frequency of the C═O stretch of the ketone is smaller, since it is an intramolecular hydrogen bond. The peak for the v_5 fundamental transition shows a small shoulder on the blue side corresponding to the non-hydrogen bonded Tt conformer. The main part of the peak is due to the more stable Tc conformer. The frequency shift between the two conformers is 23 cm^{-1} with the shoulder lying at approximately 1760 cm^{-1}. The theoretical calculations predict differences in these frequencies of 15 cm^{-1}. We note that for the matrix spectra of PA the spacing is 20.9 cm^{-1}.[4] The large absorption coefficient of the Tc conformer's carbonyl stretches obscures the smaller transition of the Tt conformer's

ketonic C═O stretching mode. The acidic C═O stretching mode is not affected by the intramolecular hydrogen bond, and our spectrum reflects this.

OH-Stretch Fundamental and Overtone Transitions. The experimental and theoretical results for the OH-stretch transitions are given in Table 3. The fundamental O−H stretching transition from the FTIR is found to lie at 3463 cm^{-1}. It is an intense feature and is in good agreement with both Hollenstein's previous work[2] and our theoretical results. The observed band shape is an off-set maximum, which Hollenstein et al. suggests as the AB band shape.[2] The fwhm is 37 cm^{-1}, which is similar to the other fundamental modes measured and can be attributed to inhomogeneous broadening. A feature to the high energy side of the OH vibrational stretch centered at 3579 cm^{-1} has been identified as the OH-stretch of the higher energy Tt conformer, which is in agreement with the calculated results (3583 cm^{-1}). The Tt conformer's OH-stretching transition has also been seen by Schellenberger et al.[3] In addition, Reva et al.[4] observed this second conformer in a low temperature argon matrix at 3556.1 cm^{-1}. Our observed feature of the Tt conformer is much smaller than the analogous Tc transition, which we primarily attribute to the large difference in the populations of the conformers. The OH-stretching fundamental transition of the Tt conformer is partially obscured by water impurity; additionally, the work of Reva et al.[4] suggests that some of the intensity at 3584 cm^{-1} is due to an overtone of the carboxylic acid carbonyl stretch of the stable conformer. This overlap precludes observing a meaningful cross section and bandwidth for the fundamental OH-stretch of the Tt conformer. Our theoretical calculations predict an integrated cross section of 1.9×10^{-17} cm/molecule for the Tc conformer's OH-stretching mode and 9.2×10^{-18} cm/molecule for the Tt conformer. This trend in the calculated cross section fits with the discussion of the hydrogen bond's effect on the dipole moment function. Our measured integrated cross section for the Tc conformer's cross section is $7.8 \pm 1.0 \times 10^{-18}$ cm/molecule.

The first overtone, $\Delta v_{OH} = 2$, is shown in Figure 3. The Tc conformer was seen at 6696 cm^{-1}, and the Tt conformer was centered at 6975 cm^{-1}. The vibrational bands of $\Delta v_{OH} = 2$ have fwhm values of 69 and 71 cm^{-1}, respectively. The increase in the width compared to the fundamental transitions (36 and 68 cm^{-1}, respectively) can be attributed to the lower intensity and inferior signal-to-noise ratio. It is apparent from Figure 3 that there is a change in the ratio of the peak areas as the integrated intensities become closer in value. The calculations suggest that this is primarily due to the larger integrated cross section for the Tt conformer compared to the Tc conformer in the $\Delta v_{OH} = 2$ transition, although a small portion may be attributed to combination bands of the Tc conformer.

As seen from the theoretical results, the fundamental for the Tc conformer has twice the cross section of the Tt conformer, while for the first overtone this relationship reverses and the integrated cross section of the Tc conformer is about one-half that of the Tt conformer. This aspect of a hydrogen bonded system has been analyzed by Kjaergaard and co-workers,[24,102,127] where the small intensity for the hydrogen bonded OH-stretching mode first overtone was attributed to the cancellation of the contributions coming from the linear and second order terms in the dipole moment function. Similar analysis was performed on the present system, and we also see the cancellation of the first two terms in the dipole moment function along the OH-stretching coordinate for the Tc conformer (see Table 7). The physical origin for this feature is still not understood.

TABLE 6: Peak Positions and Absorption Intensities Calculated by the 3D Model (B3LYP/6-31+G(d,p)

modes				
Δv_{OH}	Δv_{fb1}	Δv_{fb2}	frequency (cm^{-1})	int cross section (cm/molecule)
			Tc	
1	0	0	3445	1.96×10^{-17}
1	0	1	3697	4.04×10^{-20}
1	1	0	3830	5.76×10^{-20}
2	0	0	6702	5.25×10^{-19}
2	0	1	6953	2.26×10^{-20}
2	1	0	7084	2.21×10^{-20}
3	0	0	9774	3.32×10^{-20}
3	0	1	10025	3.26×10^{-21}
3	1	0	10152	3.31×10^{-21}
4	0	0	12663	2.58×10^{-21}
4	0	1	12916	4.58×10^{-22}
4	1	0	13038	5.19×10^{-22}
5	0	0	15401	2.64×10^{-22}
5	0	1	15655	7.25×10^{-23}
5	1	0	15774	9.31×10^{-23}
			Tt	
1	0	0	3583	1.13×10^{-17}
1	0	1	3832	9.85×10^{-22}
1	1	0	3970	2.94×10^{-21}
2	0	0	7007	8.95×10^{-19}
2	0	1	7254	1.63×10^{-22}
2	1	0	7392	7.63×10^{-23}
3	0	0	10275	5.14×10^{-20}
3	0	1	10521	7.92×10^{-23}
3	1	0	10660	4.21×10^{-23}
4	0	0	13394	4.29×10^{-21}
4	0	1	13637	1.64×10^{-23}
4	1	0	13777	6.77×10^{-24}
5	0	0	16375	4.94×10^{-22}
5	0	1	16617	3.1×10^{-24}
5	1	0	16758	1.05×10^{-24}

When a hydrogen bond is present, the first overtone transition has a larger drop in intensity compared to a free OH oscillator. As a qualitative measurement, a larger drop in the intensity corresponds to a stronger hydrogen bond. This trend was recognized in the work Kjaergaard and co-workers.[19,24] Their results illustrate that where an intramolecular hydrogen bond is present, the oscillator strength of the first OH overtone is weaker than that of its free analogue. Howard and Kjaergaard[19] suggest that the hydrogen bond becomes stronger when the carbon chain length between the alcohol groups is increased. Our PA results are consistent with those reported for ethylene glycol,[19] which also contains a hydrogen bond between adjacent carbons. The drop in intensity of the Tc conformer contrasted to the Tt conformer is further proof that the hydrogen bond is present, though relatively weak when compared to other molecules (e.g., water, 1,3-propanediol, 1,4-propanediol, glycolic acid).[18,19,24]

The third overtone of the OH vibrational stretching mode, $\Delta v_{OH} = 4$, showed a larger splitting between the two conformers than the lower transitions. The lower energy Tc-peak has dramatically broadened compared to the $\Delta v_{OH} = 1$ and 2 cases and yields a feature centered at 12 920 cm^{-1} with a fwhm of 414 cm^{-1}. The Tt-peak lies at 13 311 cm^{-1} and remains narrow with a fwhm of 56 cm^{-1}. Our theoretical predictions suggest that the cross sections for the two conformers are roughly equal so that the integrated peak areas predominantly reflect their Boltzmann populations. The integrated intensity of the Tc-peak is ~12 times that of the Tt-peak.

The fourth overtone, $\Delta v_{OH} = 5$, was only clearly observed for the Tt conformer. As seen in Figure 4, it yields a peak

TABLE 7: Contributions from the Linear, Second, and Third Order Terms of the Dipole Moment Function in the Transition Moment

	$\mu_1\langle 0\|\Delta R\|v\rangle^a$	$\mu_2\langle 0\|\Delta R^2\|v\rangle^a$	$\mu_3\langle 0\|\Delta R^3\|v\rangle^a$	sum
		Tc		
$v=1$	1.13×10^{-1}	1.55×10^{-3}	9.87×10^{-5}	1.15×10^{-1}
$v=2$	1.34×10^{-2}	-2.35×10^{-3}	-5.56×10^{-5}	1.10×10^{-2}
		Tt		
$v=1$	8.45×10^{-2}	-3.47×10^{-3}	-8.50×10^{-4}	8.02×10^{-2}
$v=2$	9.59×10^{-3}	5.57×10^{-3}	4.66×10^{-4}	1.56×10^{-2}

[a] The dipole moment function in the direction of OH is given as $\mu(R) = \mu(R_{eq}) + \Sigma_{i=1}\mu_i(R - R_{eq})^i = \mu(R_{eq}) + \Sigma_{i=1}\mu_i\Delta R^i$.

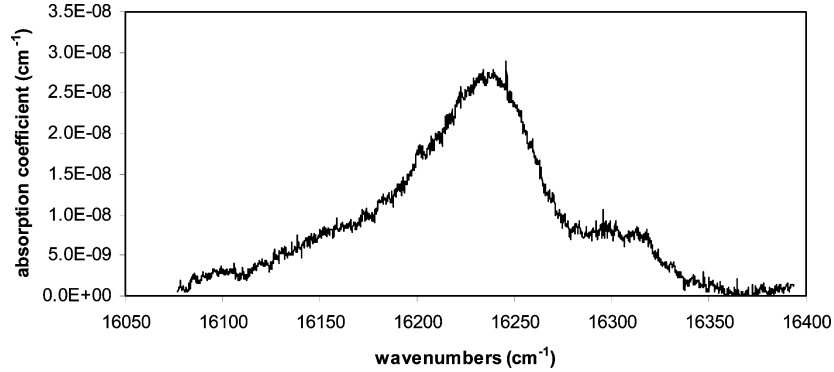

Figure 4. Observed fourth overtone of the OH-stretching mode of the Tt conformer of pyruvic acid at 355 K. The fourth overtone of the OH-stretch of the Tc conformer is too broad to be seen using our instrument.

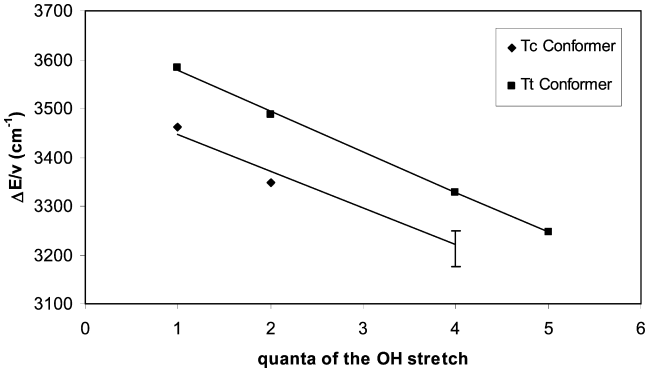

Figure 5. Birge−Sponer plots for the OH-stretching mode of the two conformers of pyruvic acid. In the Tc conformer, the $v = 4$ value is represented as a range to account for the uncertainty in the peak position.

centered at 16 237 cm^{-1} with a fwhm of 78 cm^{-1}. The Tc conformer apparently broadened massively, and it is observed only as an indistinct enhancement of the background on the low energy side of the Tt-peak.

Birge−Sponer plots of the OH-stretch transition for both conformers are presented in Figure 5. The Tt conformer gives rise to a very linear plot, with a harmonic frequency of 3743 cm^{-1} and an anharmonicity of 83 cm^{-1}, in agreement with other organic and inorganic acids studied.[18−20,48,52,53,58,65,69,70] The theoretical results for the pure OH-stretch transitions of Tt obtained with the 3D model give a harmonic frequency of 3735 cm^{-1} and an anharmonicity of 77 cm^{-1}, which is in approximate agreement with experiment. It is known that the anharmonicity calculated using the present method should be underestimated by ~10%.[123] The Birge−Sponer plot for the Tc conformer was more ill-defined, since it was difficult to uniquely determine the peak position of the broad $\Delta v_{OH} = 4$ transition. Given the uncertainty in the ν_{max} for the third overtone, we represent the frequency range between 12 700 and 13 000 cm^{-1} in Figure 5. Using the value of 12 700 cm^{-1} as the peak position, the result is a harmonic frequency of 3617 cm^{-1} and an anharmonicity of 95 cm^{-1}, which is likely an upper limit of the anharmonicity. The theoretical prediction (for which there are unique transition frequencies) gives an anharmonicity of the Tc conformer of 85 cm^{-1} which is 10% higher than for the Tt conformer.

It is useful to compare the present results for PA to the Birge−Sponer analysis of other organic compounds containing the OH-stretching mode. Organic compounds generally have an OH-stretching mode anharmonicity of between 80 and 85 cm^{-1}, similar to the Tt conformer of PA. The anharmonicity of the Tc conformer and other hydrogen bonded OH-stretches is expected to be higher than that of free OH-stretches because of the softening of the potential along the stretching coordinate. Studies of catechol and 1,4-butanediol suggest that where a strong intramolecular hydrogen bond is present, the difference between the free OH-stretching anharmonicity and that of the hydrogen bonded OH is approximately 5 cm^{-1}.[19,20] Glycolic acid (GA) is another case where intramolecular hydrogen bonding occurs and where there is an additional free OH for comparison. In GA, the anharmonicity of the acidic (free) OH-stretch is 80.3 cm^{-1} while that for the hydrogen bonded alcohol OH-stretch is 82.2 cm^{-1}.[18] The difference in anharmonicities (free versus hydrogen bonded) for GA is much smaller than that between the conformers of PA. It is interesting to note that the hydrogen bond length in Tc−PA is shorter by 0.07 Å[18,36] than its analogue in GA. Thus, it reasonable to expect that the OH-stretching potential is more highly distorted in PA and, hence, that its anharmonicity is greater. In fact, the higher OH-overtone states of Tc−PA are known[36] to be strongly affected by the proximity of a saddlepoint for the decarboxylation reaction PA → $CH_3COH + CO_2$. This would be expected to enhance the anharmonicity of Tc−PA even more compared to the apparently nonreactive conformer of GA in question.

It is interesting to review the origin of the line shape changes that are observed in the OH-stretch overtone progression. The

line widths obtained for the Tc and Tt conformers in the $\Delta v_{OH} = 1$ and 2 transitions are roughly equal and completely consistent with inhomogeneous broadening. Indeed, an earlier theoretical estimate[36] of the thermal rotational envelope is in approximate agreement with the present experiments. The profound growth of the line width for $\Delta v_{OH} = 4$ in the Tc conformer, while the Tt-peak remains narrow, suggests a homogeneous broadening mechanism that is selective to the Tc-species. In the standard interpretation of vibrational bandwidths, the homogeneous width is derived from the decay of the bright state (presumably the excited OH-stretch local mode) as a function of time. This decay, or decorrelation, can result from intramolecular energy transfer or other processes such as chemical reaction. In earlier work,[36] we clearly established that the dramatic increase in line width in Tc−PA was due to the onset of hydrogen atom chattering dynamics that occurred readily for higher overtones of Tc−PA but was absent for Tt-PA. The chattering dynamics,[78] in which the hydrogen atom undergoes fast exchange between the two oxygen atoms, was found to yield rapid decay of the initial excitation into the other vibrational modes, including the reaction coordinate. Consistent with this, there is a growth of combination bands involving the two frame bending mode that is partly responsible for the large line widths in Tc−PA. In the Tc conformer, the intensity ratio of the pure overtone to the combination band is ∼1000:1 in the fundamental region, while it drastically increases to 5:1 for the $\Delta v_{OH} = 4$ transition. It should be noted that in the Tt conformer this ratio is still small (∼100:1) even for the $\Delta v_{OH} = 5$ transition.

Combination Bands. A variety of combination bands are observed in the spectrum that have not been previously assigned. The assignments of these combination bands have been aided by the use of the relative intensity to the fundamental transitions.[2,4] It was assumed that a combination band will have very little intensity if the fundamental transition is also weak. In Table 2, we have assigned several combination bands in the range of 1000−5000 cm^{-1}. The two insets in Figure 2 show the regions where we were able to locate these low intensity transitions. The lower energy inset in Figure 2 spans the range from 1850 to 3300 cm^{-1}, and the higher energy inset encompasses 4100−4850 cm^{-1}, showing the progressions of combination bands.

Several progressions of combination bands are seen in the spectrum. One particular progression of interest is the O−H stretching mode and appears in the higher energy inset in Figure 2; the strongest of these transitions is $\upsilon_9 + \upsilon_1$ centered at 4668 cm^{-1}. The other transitions are $\upsilon_1 + \upsilon_{20}$, $\upsilon_1 + \upsilon_{11}$, $\upsilon_1 + \upsilon_{10}$, and $\upsilon_1 + \upsilon_7$, which occur at 4200, 4418, 4589, and 4851 cm^{-1}. The observation of combination bands suggests the existence of anharmonic cross terms between the two modes in the potential and/or in the dipole moment function. The appearance of combination bands also suggests a coupling of the two vibrational modes where energy can transfer. The C−C symmetric and asymmetric stretching modes also appear in combination with the OH-stretching mode in the higher energy overtones.

V. Conclusions

The vibrational spectroscopy of gas-phase PA was examined with special emphasis given to the behavior of the OH-stretching mode. The fundamental transition frequencies and the line widths are reported for 11 modes. A total of 20 combination bands were assigned. The spectrum was extended to high frequencies employing CRD spectroscopy, and the OH-stretching overtones with up to five quanta were also observed. PA proved an ideal system for studying the role of an intramolecular hydrogen bond on vibrational spectra, since two rotational conformers could be clearly observed at room temperature. The OH-stretching transitions of the non-hydrogen bonded Tt conformer behave as a typical local mode oscillator, with a linear Birge−Sponer plot and relatively narrow vibrational bandwidths. In contrast, the hydrogen bonded Tc conformer shows strong modifications in frequency, intensity, and line width due to the presence of the hydrogen bond. The pronounced differences in the line width of the two conformers' third OH-stretching overtone reveal a shortened excited-state lifetime for the Tc conformer. Our theoretical results suggest that this broadening is the result of[78] the onset of chattering motion of the hydrogen atom between the two oxygen atoms, which is not available to the Tt conformer.[18,36] We believe that changes in the O−H potential of the Tc conformer increase the anharmonicity, which is supported by the frequencies of the OH-stretch and its overtones in comparison to the Tt conformer. The high energy OH-stretching overtones absorb red light and may strongly affect the processing of PA and other organic acids in the troposphere where red light is abundant.

Acknowledgment. The authors would like to thank the Steve Brown, Karl Feierabend, and Daryl Howard for helpful discussions. We thank the National Science Foundation and CIRES for funding this research. R.T.S. and K.T. were partially supported by a grant from the Petroleum Research Fund of the American Chemical Society.

References and Notes

(1) Horowitz, A.; Meller, R.; Moortgat, G. K. *J. Photochem. Photobiol., A* **2001**, *146*, 19.
(2) Hollenstein, H.; Akermann, F.; Gunthard, H. H. *Spectrochim. Acta, Part A* **1978**, *34*, 1041.
(3) Schellenberger, A.; Beer, W.; Oehme, G. *Spectrochim. Acta* **1965**, *21*, 1345.
(4) Reva, I. D.; Stepanian, S. G.; Adamowicz, L.; Fausto, R. *J. Phys. Chem. A* **2001**, *105*, 4773.
(5) Yamamoto, S.; Back, R. A. *Can. J. Chem.* **1985**, *63*, 549.
(6) Marstokk, K. M.; Mollenda, H. *J. Mol. Struct.* **1974**, *20*, 257.
(7) Kaluza, C. E.; Bauder, A.; Gunthard, H. H. *Chem. Phys. Lett.* **1973**, *22*, 454.
(8) Kakkar, R.; Pathak, M.; Radhika, N. P. *Org. Biomol. Chem.* **2006**, *4*, 886.
(9) Kakkar, R.; Chadha, P.; Verma, D. *Internet Electron. J. Mol. Des.* **2006**, *5*, 27.
(10) Murto, J.; Raaska, T.; Kunttu, H.; Rasanen, M. *THEOCHEM* **1989**, *59*, 93.
(11) Raczynska, E. D.; Duczmal, K.; Darowska, M. *Vib. Spectrosc.* **2005**, *39*, 37.
(12) Saito, K.; Sasaki, G.; Okada, K.; Tanaka, S. *J. Phys. Chem.* **1994**, *98*, 3756.
(13) Tarakeshwar, P.; Manogaran, S. *THEOCHEM* **1998**, *430*, 51.
(14) Ellison, G. B.; Tuck, A. F.; Vaida, V. *J. Geophys. Res., [Atmos.]* **1999**, *104*, 11633.
(15) Emmeluth, C. S. M. A. L., D. *J. Chem. Phys.* **2003**, *118*, 2242.
(16) Eliason, T. L.; Havey, D. K.; Vaida, V. *Chem. Phys. Lett.* **2005**, *402*, 239.
(17) Havey, D. K.; Feierabend, K. J.; Vaida, V. *J. Phys. Chem. A* **2004**, *108*, 9069.
(18) Havey, D. K.; Feierabend, K. J.; Takahashi, K.; Skodje, R. T.; Vaida, V. *J. Phys. Chem. A* **2006**, *110*, 6439.
(19) Howard, D. L.; Kjaergaard, H. G. *J. Phys. Chem. A* **2006**, *110*, 10245.
(20) Kjaergaard, H. G.; Howard, D. L.; Schofield, D. P.; Robinson, T. W.; Ishiuchi, S.; Fujii, M. *J. Phys. Chem. A* **2002**, *106*, 258.
(21) Staikova, M.; Oh, M.; Donaldson, D. J. *J. Phys. Chem. A* **2005**, *109*, 597.
(22) Robinson, T. W.; Kjaergaard, H. G.; Ishiuchi, S.; Shinozaki, M.; Fujii, M. *J. Phys. Chem. A* **2004**, *108*, 4420.
(23) Scharge, T.; Luckhaus, D.; Suhm, M. A. *Chem. Phys.* **2008**, *346*, 167.
(24) Schofield, D. P.; Lane, J. R.; Kjaergaard, H. G. *J. Phys. Chem. A* **2007**, *111*, 567.

(25) Chaban, G. M.; Jung, J. O.; Gerber, R. B. *J. Phys. Chem. A* **2000**, *104*, 2772.
(26) Chaban, G. M.; Xantheas, S. S.; Gerber, R. B. *J. Phys. Chem. A* **2003**, *107*, 4952.
(27) von Helden, G.; Compagnon, I.; Blom, M. N.; Frankowski, M.; Erlekam, U.; Oomens, J.; Brauer, B.; Gerber, R. B.; Meijer, G. *Phys. Chem. Chem. Phys.* **2008**, *10*, 1248.
(28) Garden, A. L.; Halonen, L.; Kjaergaard, H. G. *J. Phys. Chem. A* **2008**, *112*, 7439.
(29) Child, M. S.; Halonen, L. *Adv. Chem. Phys.* **1984**, *57*, 1.
(30) Henry, B. R. *Acc. Chem. Res.* **1977**, *10*, 207.
(31) Henry, B. R. *Acc. Chem. Res.* **1987**, *20*, 429.
(32) Quack, M. *Annu. Rev. Phys. Chem.* **1990**, *41*, 839.
(33) Henry, B. R.; Kjaergaard, H. G. *Can. J. Chem.* **2002**, *80*, 1635.
(34) Huang, C. L.; Wu, C. C.; Lien, M. H. *J. Phys. Chem. A* **1997**, *101*, 7867.
(35) Dunn, M. E. S., G. C.; Vaida, V. *J. Phys. Chem. A* **2008**, *112*, 10226.
(36) Takahashi, K.; Plath, K. L.; Vaida, V.; Skodje, R. T. *J. Phys. Chem. A* **2008**, *112*, 7321.
(37) Baklanov, A. V.; Aldener, M.; Lindgren, B.; Sassenberg, U. *J. Chem. Phys.* **2000**, *112*, 6649.
(38) Bar, I.; Rosenwaks, S. *Int. Rev. Phys. Chem.* **2001**, *20*, 711.
(39) Barnes, R. J.; Sinha, A. *J. Chem. Phys.* **1997**, *107*, 3730.
(40) Brown, S. S.; Wilson, R. W.; Ravishankara, A. R. *J. Phys. Chem. A* **2000**, *104*, 4976.
(41) Callegari, A.; Rizzo, T. R. *Chem. Soc. Rev.* **2001**, *30*, 214.
(42) Crim, F. F. *Annu. Rev. Phys. Chem.* **1984**, *35*, 657.
(43) Crim, F. F. *J. Phys. Chem.* **1996**, *100*, 12725.
(44) Crim, F. F. *Acc. Chem. Res.* **1999**, *32*, 877.
(45) Donaldson, D. J.; Frost, G. J.; Rosenlof, K. H.; Tuck, A. F.; Vaida, V. *Geophys. Res. Lett.* **1997**, *24*, 2651.
(46) Donaldson, D. J.; Orlando, J. J.; Amann, S.; Tyndall, G. S.; Proos, R. J.; Henry, B. R.; Vaida, V. *J. Phys. Chem. A* **1998**, *102*, 5171.
(47) Donaldson, D. J.; Tuck, A. F.; Vaida, V. *Chem. Rev.* **2003**, *103*, 4717.
(48) Feierabend, K. J.; Havey, D. K.; Brown, S. S.; Vaida, V. *Chem. Phys. Lett.* **2006**, *420*, 438.
(49) Feierabend, K. J.; Havey, D. K.; Vaida, V. *Spectrochim. Acta, Part A* **2004**, *60*, 2775.
(50) Fleming, P. R.; Li, M. Y.; Rizzo, T. R. *J. Chem. Phys.* **1991**, *94*, 2425.
(51) Fono, L.; Donaldson, D. J.; Proos, R. J.; Henry, B. R. *Chem. Phys. Lett.* **1999**, *311*, 131.
(52) Havey, D. K.; Vaida, V. *J. Mol. Spectrosc.* **2004**, *228*, 152.
(53) Haynes, L. M.; Vogelhuber, K. M.; Pippen, J. L.; Hsieh, S. *J. Chem. Phys.* **2005**, 123.
(54) Hintze, P. E.; Feierabend, K. J.; Havey, D. K.; Vaida, V. *Spectrochim. Acta, Part A* **2005**, *61*, 559.
(55) Hintze, P. E.; Kjaergaard, H. G.; Vaida, V.; Burkholder, J. B. *J. Phys. Chem. A* **2003**, *107*, 1112.
(56) Holland, S. M.; Stickland, R. J.; Ashfold, M. N. R.; Newnham, D. A.; Mills, I. M. *J. Chem. Soc., Faraday Trans.* **1991**, *87*, 3461.
(57) Homitsky, S. C.; Dragulin, S. M.; Haynes, L. M.; Hsieh, S. *J. Phys. Chem. A* **2004**, *108*, 9492.
(58) Ishiuchi, S.; Fujii, M.; Robinson, T. W.; Miller, B. J.; Kjaergaard, H. G. *J. Phys. Chem. A* **2006**, *110*, 7345.
(59) Konen, I. M.; Li, E. X. J.; Lester, M. I.; Vazquez, J.; Stanton, J. F. *J. Chem. Phys.* **2006**, 125.
(60) Lane, J. R.; Kjaergaard, H. G.; Plath, K. L.; Vaida, V. *J. Phys. Chem. A* **2007**, *111*, 5434.
(61) Lange, K. R.; Wells, N. P.; Plegge, K. S.; Phillips, J. A. *J. Phys. Chem. A* **2001**, *105*, 3481.
(62) Matthews, J.; Sharma, R.; Sinha, A. *J. Phys. Chem. A* **2004**, *108*, 8134.
(63) Matthews, J.; Sinha, A.; Francisco, J. S. *J. Chem. Phys.* **2004**, *120*, 10543.
(64) Nizkorodov, S. A.; Crounse, J. D.; Fry, J. L.; Roehl, C. M.; Wennberg, P. O. *Atmos. Chem. Phys.* **2005**, *5*, 385.
(65) Phillips, J. A.; Orlando, J. J.; Tyndall, G. S.; Vaida, V. *Chem. Phys. Lett.* **1998**, *296*, 377.
(66) Reiche, F.; Abel, B.; Beck, R. D.; Rizzo, T. R. *J. Chem. Phys.* **2000**, *112*, 8885.
(67) Rizzo, T. R.; Hayden, C. C.; Crim, F. F. *Faraday Discuss.* **1983**, *75*, 223.
(68) Roehl, C. M.; Nizkorodov, S. A.; Zhang, H.; Blake, G. A.; Wennberg, P. O. *J. Phys. Chem. A* **2002**, *106*, 3766.
(69) Rontu, N.; Vaida, V. *J. Mol. Spectrosc.* **2006**, *237*, 19.
(70) Rontu, N.; Vaida, V. *J. Phys. Chem. B* **2008**, *112*, 276.
(71) Salawitch, R. J.; Wennberg, P. O.; Toon, G. C.; Sen, B.; Blavier, J. F. *Geophys. Res. Lett.* **2002**, 29.
(72) Sibert, E. L.; Reinhardt, W. P.; Hynes, J. T. *J. Chem. Phys.* **1982**, *77*, 3583.
(73) Uzer, T.; Hynes, J. T.; Reinhardt, W. P. *J. Chem. Phys.* **1986**, *85*, 5791.
(74) Vaida, V.; Kjaergaard, H. G.; Hintze, P. E.; Donaldson, D. J. *Science* **2003**, *299*, 1566.
(75) Wennberg, P. O.; Salawitch, R. J.; Donaldson, D. J.; Hanisco, T. F.; Lanzendorf, E. J.; Perkins, K. K.; Lloyd, S. A.; Vaida, V.; Gao, R. S.; Hintsa, E. J.; Cohen, R. C.; Swartz, W. H.; Kusterer, T. L.; Anderson, D. E. *Geophys. Res. Lett.* **1999**, *26*, 1373.
(76) Zhang, H.; Roehl, C. M.; Sander, S. P.; Wennberg, P. O. *J. Geophys. Res., [Atmos.]* **2000**, *105*, 14593.
(77) Kjaergaard, H. G.; Lane, J. R.; Garden, A. L.; Scholfield, D. P.; Robinson, T. W.; Mills, J. M. *Adv. Quantum Chem.* **2008**, *55*, 137.
(78) Skodje, R. T. *Annu. Rev. Phys. Chem.* **1993**, *44*, 145.
(79) Andreae, M. O.; Talbot, R. W.; Li, S. M. *J. Geophys. Res., [Atmos.]* **1987**, *92*, 6635.
(80) Baboukas, E. D.; Kanakidou, M.; Mihalopoulos, N. *J. Geophys. Res., [Atmos.]* **2000**, *105*, 14459.
(81) Fisseha, R.; Dommen, J.; Sax, M.; Paulsen, D.; Kalberer, M.; Maurer, R.; Hofler, F.; Weingartner, E.; Baltensperger, U. *Anal. Chem.* **2004**, *76*, 6535.
(82) Kawamura, K.; Imai, Y.; Barrie, L. A. *Atmos. Environ.* **2005**, *39*, 599.
(83) Kawamura, K.; Yasui, O. *Atmos. Environ.* **2005**, *39*, 1945.
(84) Miller, W. L.; Zepp, R. G. *Geophys. Res. Lett.* **1995**, *22*, 417.
(85) Moran, M. A.; Zepp, R. G. *Limnol. Oceanogr.* **1997**, *42*, 1307.
(86) Talbot, R. W.; Andreae, M. O.; Berresheim, H.; Jacob, D. J.; Beecher, K. M. *J. Geophys. Res., [Atmos.]* **1990**, *95*, 16799.
(87) Ervens, B.; Feingold, G.; Frost, G. J.; Kreidenweis, S. M. *J. Geophys. Res., [Atmos.]* **2004**, 109.
(88) Guzman, M. I.; Colussi, A. I.; Hoffmann, M. R. *J. Phys. Chem. A* **2006**, *110*, 3619.
(89) Mellouki, A.; Mu, Y. J. *J. Photochem. Photobiol., A* **2003**, *157*, 295.
(90) Dhanya, S.; Maity, D. K.; Upadhyaya, H. P.; Kumar, A.; Naik, P. D.; Saini, R. D. *J. Chem. Phys.* **2003**, *118*, 10093.
(91) Colberg, M. R.; Watkins, R. J.; Krogh, O. D. *J. Phys. Chem.* **1984**, *88*, 2817.
(92) Rosenfeld, R. N.; Weiner, B. *J. Am. Chem. Soc.* **1983**, *105*, 3485.
(93) Hall, G. E.; Muckerman, J. T.; Preses, J. M.; Weston, R. E.; Flynn, G. W. *Chem. Phys. Lett.* **1992**, *193*, 77.
(94) Taylor, R. *Int. J. Chem. Kinet.* **1987**, *19*, 709.
(95) Buechele, J. L.; Weitz, E.; Lewis, F. D. *Chem. Phys. Lett.* **1981**, *77*, 280.
(96) Carlton, A. G.; Turpin, B. J.; Lim, H. J.; Altieri, K. E.; Seitzinger, S. *Geophys. Res. Lett.* **2006**, 33.
(97) Heald, C. L.; Jacob, D. J.; Park, R. J.; Russell, L. M.; Huebert, B. J.; Seinfeld, J. H.; Liao, H.; Weber, R. J. *Geophys. Res. Lett.* **2005**, 32.
(98) Kanakidou, M.; Seinfeld, J. H.; Pandis, S. N.; Barnes, I.; Dentener, F. J.; Facchini, M. C.; Van Dingenen, R.; Ervens, B.; Nenes, A.; Nielsen, C. J.; Swietlicki, E.; Putaud, J. P.; Balkanski, Y.; Fuzzi, S.; Horth, J.; Moortgat, G. K.; Winterhalter, R.; Myhre, C. E. L.; Tsigaridis, K.; Vignati, E.; Stephanou, E. G.; Wilson, J. *Atmos. Chem. Phys.* **2005**, *5*, 1053.
(99) Molina, M. J.; Ivanov, A. V.; Trakhtenberg, S.; Molina, L. T. *Geophys. Res. Lett.* **2004**, 31.
(100) Volkamer, R.; Jimenez, J. L.; San Martini, F.; Dzepina, K.; Zhang, Q.; Salcedo, D.; Molina, L. T.; Worsnop, D. R.; Molina, M. J. *Geophys. Res. Lett.* **2006**, 33.
(101) Warneck, P. *Atmos. Environ.* **2003**, *37*, 2423.
(102) Kjaergaard, H. G.; Low, G. R.; Robinson, T. W.; Howard, D. L. *J. Phys. Chem. A* **2002**, *106*, 8955.
(103) Staikova, M.; Donaldson, D. J. *Phys. Chem. Earth, Part C: Sol.−Terr. Planet. Sci.* **2001**, *26*, 473.
(104) Vaida, V.; Kjaergaard, H. G.; Feierabend, K. J. *Int. Rev. Phys. Chem.* **2003**, *22*, 203.
(105) Takahashi, K.; Kramer, Z. C.; Vaida, V.; Skodje, R. T. *Phys. Chem. Chem. Phys.* **2007**, *9*, 3864.
(106) Luc, P.; Gerstenkorn, S. *Appl. Opt.* **1978**, *17*, 1327.
(107) Richard, E. C.; Vaida, V. *J. Chem. Phys.* **1991**, *94*, 153.
(108) Berden, G.; Peeters, R.; Meijer, G. *Int. Rev. Phys. Chem.* **2000**, *19*, 565.
(109) Brown, S. S. *Chem. Rev.* **2003**, *103*, 5219.
(110) McDonald, R. A.; Shrader, S. A.; Stull, D. R. *J. Chem. Eng. Data* **1959**, *4*, 311.
(111) Stull, D. R. *J. Ind. Eng. Chem.* **1947**, *39*, 517.
(112) Becke, A. D. *J. Chem. Phys.* **1993**, *98*, 5648.
(113) Lee, C. T.; Yang, W. T.; Parr, R. G. *Phys. Rev. B* **1988**, *37*, 785.
(114) Clark, T.; Chandrasekhar, J.; Spitznagel, G. W.; Schleyer, P. V. *J. Comput. Chem.* **1983**, *4*, 294.
(115) Frisch, M. J.; Pople, J. A.; Binkley, J. S. *J. Chem. Phys.* **1984**, *80*, 3265.
(116) Frisch, M. J. T., G. W.; Schlegel, H. B.; Scuseria, G. E.; Robb, M. A.; Cheeseman, J. R.; Montgomery, J. A., Jr.; Vreven, T.; Kudin, K. N.; Burant, J. C.; Millam, J. M.; Iyengar, S. S.; Tomasi, J.; Barone, V.;

Mennucci, B.; Cossi, M.; Scalmani, G.; Rega, N.; Petersson, G. A.; Nakatsuji, H.; Hada, M.; Ehara, M.; Toyota, K.; Fukuda, R.; Hasegawa, J.; Ishida, M.; Nakajima, T.; Honda, Y.; Kitao, O.; Nakai, H.; Klene, M.; Li, X.; Knox, J. E.; Hratchian, H. P.; Cross, J. B.; Adamo, C.; Jaramillo, J.; Gomperts, R.; Stratmann, R. E.; Yazyev, O.; Austin, A. J.; Cammi, R.; Pomelli, C.; Ochterski, J. W.; Ayala, P. Y.; Morokuma, K.; Voth, G. A.; Salvador, P.; Dannenberg, J. J.; Zakrzewski, V. G.; Dapprich, S.; Daniels, A. D.; Strain, M. C.; Farkas, O.; Malick, D. K.; Rabuck, A. D.; Raghavachari, K.; Foresman, B.; Liu, G.; Liashenko, A.; Piskorz, P.; Komaromi, I.; Martin, R. L.; Fox, D. J.; Keith, T.; Al-Laham, M. A.; Peng, C. Y.; Nanayakkar, A.; Challacombe, M.; Gill, P. M. W.; Johnson, B.; Chen, W.; Wong, M. W.; Gonzalez, C.; Pople, J. A., *Gaussian 03*, revision C.02 ed.; Gaussian, Inc.: Wallingford, CT, 2004.

(117) Krishnan, R.; Binkley, J. S.; Seeger, R.; Pople, J. A. *J. Chem. Phys.* **1980**, *72*, 650.

(118) McLean, A. D.; Chandler, G. S. *J. Chem. Phys.* **1980**, *72*, 5639.

(119) Moller, C.; Plesset, M. S. *Phys. Rev.* **1934**, *46*, 0618.

(120) Woon, D. E.; Dunning, T. H. *J. Chem. Phys.* **1993**, *98*, 1358.

(121) Dunning, T. H. *J. Chem. Phys.* **1989**, *90*, 1007.

(122) Kendall, R. A.; Dunning, T. H.; Harrison, R. J. *J. Chem. Phys.* **1992**, *96*, 6796.

(123) Takahashi, K. S. M. Y. S. *J. Phys. Chem. A* **2003**, *107*, 11092.

(124) Kjaergaard, H. G.; Goddard, J. D.; Henry, B. R. *J. Chem. Phys.* **1991**, *95*, 5556.

(125) Kjaergaard, H. G.; Turnbull, D. M.; Henry, B. R. *J. Chem. Phys.* **1993**, *99*, 9438.

(126) Niefer, B. I.; Kjaergaard, H. G.; Henry, B. R. *J. Chem. Phys.* **1993**, *99*, 5682.

(127) Howard, D. L.; Jrgensen, P.; Kjaergaard, H. G. *J. Am. Chem. Soc.* **2005**, *127*, 17096.

(128) Purvis, G. D.; Bartlett, R. J. *J. Chem. Phys.* **1982**, *76*, 1910.

(129) Raghavachari, K.; Trucks, G. W.; Pople, J. A.; Headgordon, M. *Chem. Phys. Lett.* **1989**, *157*, 479.

(130) Werner, H.-J. K., P. J.; Lindh, R.; Schutz, M.; Celani, P.; Korona, R.; Manby, F. R.; Rauhut, G.; Amos, R. D.; Bernharsson, A.; Berning, A.; Cooper, D. L.; Deegan, M. J. O.; Dobbyn, A. J.; Eckert, F.; Nicklass, A.; Palmieri, P.; Pitzer, R.; Schumann, U.; Stoll, H.; Stone, A. J.; Tarroni, R.; Thorsteinsson, T. *MOLPRO: a package of ab initio programs*, 2002.6 ed.; Birmingham, U.K., 2003.

(131) Pimentel, G. C. M.; Aubrey, L. *The Hydrogen Bond*; W. H. Freeman and Company: San Francisco, CA, 1960.

JP810687T